ARTICLES

Triplet Energy Migration among Energetically Disordered Chromophores in Polymer Matrixes. 2. Thermally Induced Supertrap Formation

Kenji Hisada,† Shinzaburo Ito, and Masahide Yamamoto*

Department of Polymer Chemistry, Graduate School of Engineering, Kyoto University, Sakyo-ku, Kyoto 606-8501, Japan

Received: December 11, 1997; In Final Form: March 26, 1998

Triplet energy migration in poly[(9-phenanthrylmethyl methacrylate)-*co*-(methyl methacrylate)] films has been investigated by phosphorescence spectroscopy. Phosphorescence spectra from *triplet trap sites* were slightly shifted toward the low-energy side with a rise in temperature. The energy migration rates in these systems are complicated, since the trap sites have various energy levels depending on the amplitude of interaction energies. The kinetic analysis was made on the basis of Bässler's model in which the site energies have a Gaussian distribution. The fitting procedure well reproduced the phosphorescence decay data in the temperature range 15−100 K, indicating that the concentration of the supertrap increased steeply with the motion of the matrix polymer.

Introduction

Light-induced processes in aromatic polymers have been well investigated over the past two decades.[1−6] One of the important processes is the excitation energy migration in polymers through the aromatic pendant groups. The electronic excited state of a chromophore moves to the adjacent chromophore sites by the Förster or Dexter mechanism.[7,8] The Dexter-type energy transfer is often utilized in photosensitive polymers in view of the long lifetime of the triplet state. However, the behavior of triplet energy transfer in polymers has not been fully elucidated because of experimental difficulties such as weak emission due to efficient nonradiative deactivation. The triplet energy migration involves a short-range interaction of chromophores with the overlapping of electronic charge clouds.[8] This means that the efficient transport of triplet excitons occurs only in concentrated chromophoric systems. In such systems, excited chromophores often form stabilized sites such as an excimer site or a trap site.[9−14]

The interaction between chromophores in polymer films is classified into two types: *excimer-type* and *trap-type*.[15−18] In copolymers with high concentrations of phenanthrene or naphthalene chromophores, the films show slightly red-shifted phosphorescence spectra maintaining the vibrational band structure compared with the films having a low concentration of chromophores.[15,17] This type of excited species is termed a *triplet trap site* (^{3}T*) to distinguish it from the *triplet excimer*, which is often observed in the copolymer films containing carbazole or benzene chromophores.[16,18] The ^{3}T* sites act as shallow traps for energy migration. The decay profiles of phosphorescence from ^{3}T* sites are characterized by multiexponential functions or stretched exponential functions.

Many workers have proposed models to describe the complicated relaxation process of excited states.[19−29] Transport properties in inhomogeneous systems are described by a distribution of microscopic (site-to-site) transfer rates (temporal disorder) and by dispersive magnitudes of interactions with the surroundings (energetic disorder). Spatial randomness may be modeled by fractals,[30,31] and temporal disorder can be accounted for by using a waiting-time distribution, as in continuous-time random walk (CTRW),[32,33] and multiple trapping (MT)[33,34] approaches. A drastic temperature effect on excitation energy migration and trapping could not be explained by either CTRW or MT models. Bässler et al. analyzed the migration process of triplet excitons in organic matrixes by Monte Carlo simulation.[35] They assumed that the distribution of site energies (DOS) is expressed by a Gaussian function and that an exciton hops among these sites. They also reported that this DOS model is also adequate for expressing the electron transport, photophysical hole burning, singlet energy migration, and thermally induced transformation of spiropyran in polymer solids.[36,37] We have applied this model to chromophoric polymer systems, and the phosphorescence decay profiles were successfully represented in a temperature range 115−165 K.[38] In a previous study, we observed the spectral shift of phosphorescence for the copolymer films containing phenanthrene chromophores.[39] The spectral shift was simulated by the Monte Carlo method, and the DOS of ^{3}T* was obtained in a temperature range of 15−100 K. Bässler et al. assumed that the dispersity of DOS is independent of temperature. However, in a soft matrix such as organic polymers, the dispersity seems to vary with temperature. The experimental spectral shift can be reproduced by the Monte Carlo simulation when the dispersity was enlarged with temperature. The temperature dependence of the dispersity of DOS is mainly attributed to the homogeneous broadening. In the present study, we investigated the phosphorescence decay

† Present address is Department of Applied Chemistry and Biotechnology, Faculty of Engineering, Fukui University, 3-9-1 Bunkyo, Fukui 910-8507, Japan.

S1089-5647(98)00508-2 CCC: $15.00
Published on Web 05/02/1998

TABLE 1: Compositions (*x*), Molecular Weights of P(PhenMMA-*co*-MMA)s, Chromophore Concentrations ([Phen]), and Average Distances between Phenanthrene Chromophores (*D*) in the Films

sample	*x* mol %	MW[a]	10^5[Phen] mol L^{-1}	*D*[b] nm
P(PhenMMA-*co*-MMA)L	0.78	1.30	0.09	2.63
P(PhenMMA-*co*-MMA)H	18.6	1.20	1.67	1.00

[a] Determined by GPC calibrated with polystyrene standards. [b] Calculated by $D = n^{-(1/3)}$, where *n* is the average number of chromophores per unit volume.

profiles of poly[(9-phenanthrylmethyl methacrylate)-*co*-(methyl methacrylate)] (P(PhenMMA-*co*-MMA)) films with and without acceptor. The fitting procedure of the decay curves allowed us to evaluate the concentration of supertraps, which are the quenching sites of the trap-site phosphorescence of P(PhenMMA-*co*-MMA). The relationship between the concentration of the supertrap and the molecular motion of the matrix polymer is discussed in terms of the results from measurements of the capacitance and conductance of the copolymer films.

Experimental Section

Materials. Synthetic methods for P(PhenMMA-*co*-MMA) were described previously.[15] The properties of copolymers are listed in Table 1. 1,4-Dibromonaphthalene (DBN; Tokyo Chemical Industry Co., Ltd.) was recrystallized from methanol, which was used as a triplet energy acceptor. The energy level for the lowest singlet state of DBN is higher than that of phenanthrene (Phen) i.e., when Phen is selectively excited at 337 nm, only the triplet state of Phen is quenched by DBN.[38]

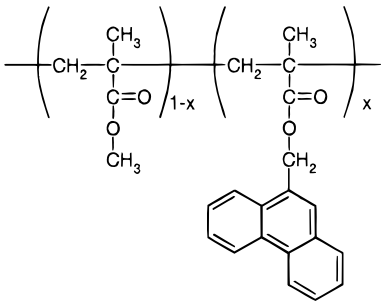

Sample Preparation. A solid film on a quartz plate was formed by casting a solution of the copolymer in a small quantity of 1,2-dichloroethane (spectrophotomeric grade; Dojindo Laboratories). After the solvent evaporated, the film was dried in vacuo for more than 10 h at room temperature and at 110 °C, respectively. The drying process was continued until the solvent could not be detected by UV spectrometry or IR spectrometry. In the same manner, DBN-doped film was prepared by addition of prescribed amounts of DBN to the casting solution.

Measurements. Steady-state emission spectra were recorded with a Hitachi model 850 spectrofluorophotometer. Phosphorescence decay curves and time-resolved phosphorescence spectra were measured with a phosphorimeter assembled in our laboratory. A xenon flash lamp (EG&G, FX198UV) and a nitrogen laser (NDH Co., JH-500) were used as the pulsed excitation light sources for the measurements in millisecond and microsecond time regions, respectively. Details of the system have been described elsewhere.[16] In the spectroscopic measurement, the temperature of the polymer film was varied by a closed-cycle helium system (Iwatani plantech Co., CRT 510). The temperature was maintained within ±0.1 K by a temperature control unit (Iwatani plantech Co., TCU-4). The temperature of the sample was monitored by a calibrated thermocouple (Au + 0.07% Fe/chromel) connected to a copper block in the neighborhood of the sample to provide a temperature as close to the area of observation as possible. Details of the temperature-controlling system for the spectroscopic measurements have been described previously.[39]

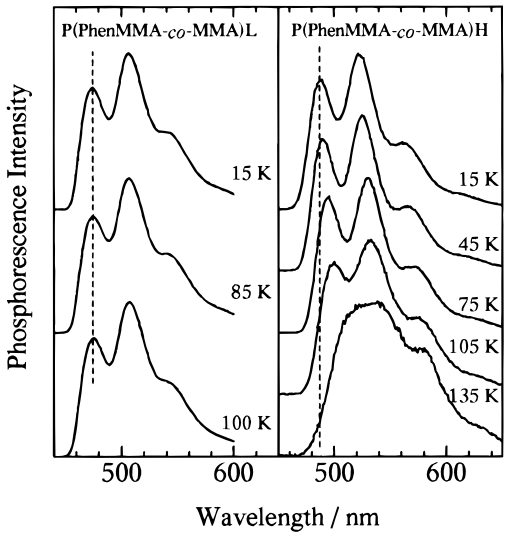

Figure 1. (A, left) Phosphorescence spectra of P(PhenMMA-*co*-MMA)L film at three different temperatures. (B, right) Phosphorescence spectra of P(PhenMMA-*co*-MMA)H film in which the sample temperature was changed from 15 (top) to 135 K (bottom) by 30 K separations. Both samples were excited at 337 nm, and the spectra are uncorrected for instrumental response.

For measurements of the capacitance and conductance of films, a three-electrode method was employed with a precision LCR meter (ANDO Co., AG-4311B). Frequencies ranging from 100 Hz to 100 kHz were covered. The sample temperature was varied by a closed-cycle liquid helium system (Daikin Co., CRYOKELVIN 204SC) between 15 K and room temperature. Measurements of capacitance and conductance were made by maintaining the elevating rate at 1−3 K min^{-1}.

Results and Discussion

Spectroscopic Measurements. The temperature dependence of phosphorescence spectra for P(PhenMMA-*co*-MMA) films is shown in Figure 1. In the abbreviations L and H of the samples refer to low and high relative mole fractions of the Phen chromophore in the polymer (see Table 1). The phosphorescence spectra of P(PhenMMA-*co*-MMA)L film were independent of temperature. On the other hand, for the P(PhenMMA-*co*-MMA)H film, the spectra were shifted to longer wavelengths and the intensity decreased with an increase of temperature, but the band shape remained the same below 105 K. The result shows that the chromophores form more stabilized ^{3}T* sites within their excited lifetimes for the polymer having a higher concentration of chromophores. The broadened spectra at high temperatures may be caused by overlapping of the emission from several ^{3}T* sites of different energy levels. In the previous study, a Monte Carlo simulation of the spectral shift revealed the growth of interchromophore interaction as the enlargement of the energy dispersity of the triplet site.[39] Table 2 shows the dispersion parameters α and σ defined in the later section.

Figure 2 depicts the phosphorescence spectra for a P(PhenMMA-*co*-MMA)H film containing a small amount of DBN (5×10^{-3} mol L^{-1}). The concentration of DBN is ca. $^1/_{300}$ of that

TABLE 2: Standard Deviation of the Trap Energy Distribution (σ) and Dispersion Parameter (α) for P(PhenMMA-*co*-MMA)H Film and the Lifetime of Dibromonaphthalene (τ_a) in PMMA

temp/K	σ/cm^{-1}	α^a	τ_a/ms
15	145	0.076	4.5
30	155	0.23	4.4
45	180	0.33	4.3
60	210	0.39	4.3
75	260	0.39	4.2
85	290	0.40	4.2
90	305	0.40	4.1
95	325	0.40	4.1
100	340	0.40	4.1

[a] $\alpha^{-1} = [\sigma/(4kT)]^2 + 1$.

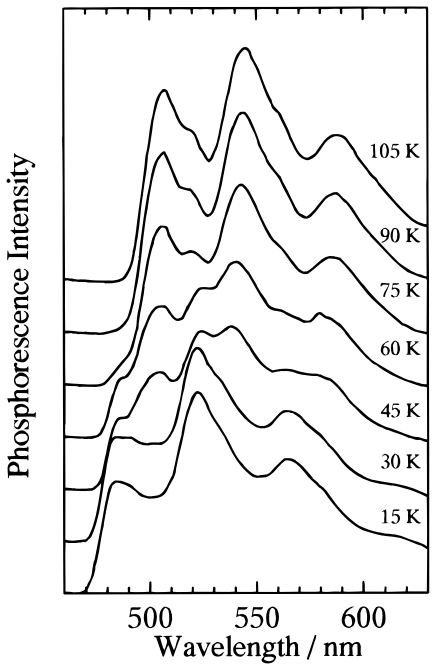

Figure 2. Phosphorescence spectra of the DBN-doped P(PhenMMA-*co*-MMA)H film excited at 335 nm. Sample temperature was changed from 15 (bottom) to 105 K (top) by 15 K separations.

of Phen. At 15 K, the phosphorescence from only the phenanthrene unit at 485, 522, and 564 nm was observed. The Phen phosphorescence decreased with a rise in temperature, and in place of it, the DBN phosphorescence appeared at 507, 545, and 588 nm. In the P(PhenMMA-*co*-MMA)H film, iterative trapping−detrapping at ^{3}T* sites and capture of the exciton to DBN result in a preferential loss of high-energy emission from these ^{3}T* sites. At higher temperatures, the probability that the exciton reaches more stabilized sites or an acceptor site increases by the activation of detrapping process.[15] When DBN was doped in a P(PhenMMA-*co*-MMA)L film in which energy migration could not occur, only Phen phosphorescence was observed.

Figure 3 shows phosphorescence decay profiles of a P(PhenMMA-*co*-MMA)H film at various temperatures. The decay curves were almost single-exponential below 45 K. Above 60 K, the decay profiles became multiexponential (more than two) and the decay rate increased. For the P(PhenMMA-*co*-MMA)L film, the decay curves were single-exponential in the same temperature range.

The decay curves of the P(PhenMMA-*co*-MMA) film were fitted by a biexponential function (eq 1),

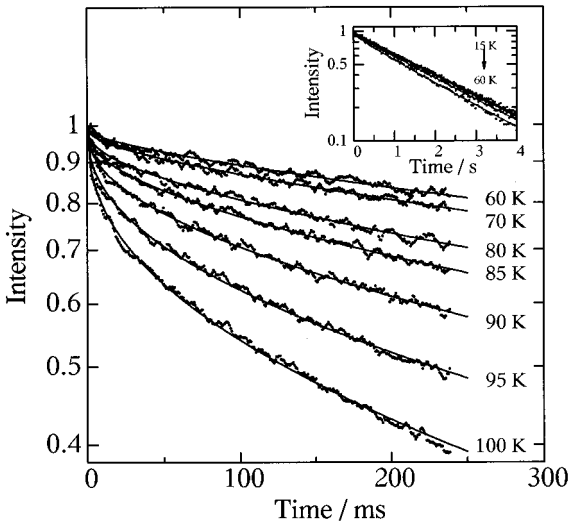

Figure 3. Temperature dependence of decay curves of phenanthrene phosphorescence in P(PhenMMA-*co*-MMA)H film. The emission was detected at 545 nm. The solid lines represent the results of calculation based on the DOS model with $\nu_0 = 1.39 \times 10^5$ ms^{-1} and $\alpha = 0.076$ (15 K), 0.23 (30 K), 0.33 (45 K), 0.39 (60 K), 0.39 (75 K), 0.40 (85 K), 0.40 (90 K), 0.40 (95 K), and 0.40 (100 K).

$$I_d(t) = I_d(0)[F \exp(-t/\tau_1) + (1 - F) \exp(-t/\tau_2)] \quad (1)$$

and the average lifetime of the phenanthrene triplet, $\langle\tau\rangle$, was calculated by eq 2.

$$\langle\tau\rangle = F\tau_1 + (1 - F)\tau_2 \quad (2)$$

The temperature dependence of $\langle\tau\rangle$ is shown in Figure 4. For P(PhenMMA-*co*-MMA)H film, $\langle\tau\rangle$ decreased rapidly above 50 K, while $\langle\tau\rangle$ was almost constant for the P(PhenMMA-*co*-MMA)L film. This indicates that the energy migration to some quenching sites is responsible for this behavior. We will refer to this quenching site as a supertrap.

Figure 5 shows the rise and decay profiles of the acceptor (DBN) phosphorescence in the P(PhenMMA-*co*-MMA)H film at various temperatures. The rise component becames larger and the rise peak was delayed with increasing temperature. The behavior of phosphorescence spectra and its decay profiles can be interpreted by a thermally accelerated process as shown in Figure 6. The migrating exciton is captured by a ^{3}T* site, which has a potential energy lower than the surrounding sites. At lower temperatures, the triplet exciton cannot overcome the energy barrier so that it is captured immediately and migrates within a narrow range of sites. At higher temperatures, the exciton may overcome the barrier and migrates over a wide range of sites. Therefore, the probability that the triplet exciton reaches a supertrap or an acceptor site increases with the elevation of temperature.

Computer Simulation. For a P(PhenMMA-*co*-MMA) film without an acceptor, the equation for the excited triplet phenanthrene chromophore is given by

$$dD(t)/dt = -(\tau_d^{-1} + c_E\nu(t))D(t) \quad (3)$$

where $D(t)$ is the number of excited chromophores, $\nu(t)$ is the exciton hopping frequency at time t, c_E is the concentration of the supertrap, and τ_d is the intrinsic lifetime of the Phen chromophore. Bässler et al. analyzed the triplet energy migration in amorphous organic layers. They assumed that the energy migration occurs through exciton hopping among the sites that exhibit a Gaussian DOS. By a Monte Carlo simulation,[37] the

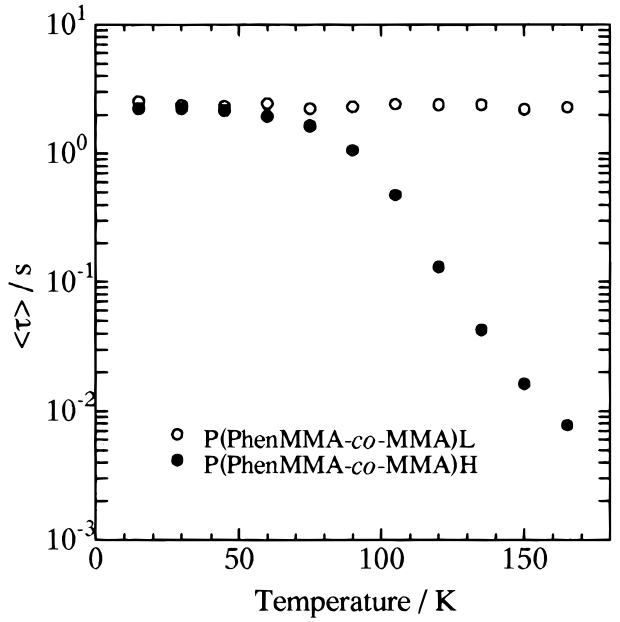

Figure 4. Temperature dependence of average lifetime of phosphorescence $\langle\tau\rangle$: (○) P(PhenMMA-*co*-MMA)L film; (●) P(PhenMMA-*co*-MMA)H film.

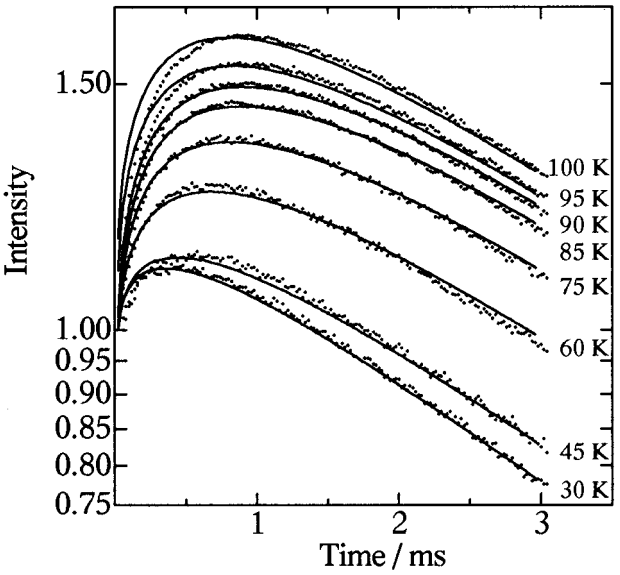

Figure 5. Temperature dependence of rise and decay curves of DBN phosphorescence in P(PhenMMA-*co*-MMA)H film. The emission was detected at 545 nm. The solid lines represent the results of calculations based on the DOS model. The parameters of each temperature are identical to those in Figure 3.

time dependence of $\nu(t)$ is obtained as follows:

$$\nu(t) = \nu_0(t/t_0)^{\alpha-1} \tag{4}$$

where ν_0 and t_0 are the jump frequency and jump time, respectively, in an energetically discrete hopping system and α is the dispersion parameter. Empirically, α is predicted to follow the relation

$$\alpha^{-1} = \left(\frac{\sigma}{4kT}\right)^2 + 1 \tag{5}$$

where σ is the width of the Gaussian distribution.[36] Then we obtained $D(t)$ from eqs 3 and 4 as follows.

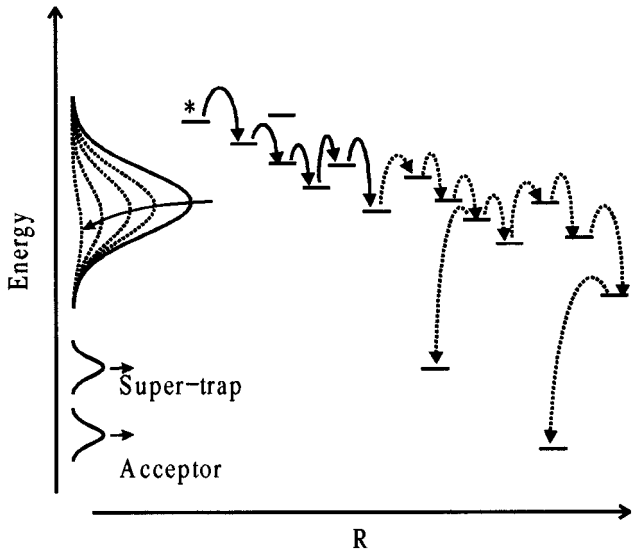

Figure 6. Schematic illustration of the energy migration among the levels with Gaussian energy distribution. The full curves indicate the density of state profile. Dashed curves map the distribution of excitons (*) after the excitation, which populates a small fraction of sites randomly. At low temperatures, an exciton is trapped by a shallow ^{3}T* site. With an increase of temperature, the exciton migrates to a supertrap or an acceptor site.

$$D(t) = D(0)\exp\left(\frac{-c_E B t^\alpha}{\alpha} - \frac{t}{\tau_d}\right) \tag{6}$$

where

$$B = \nu_0 {t_0}^{1-\alpha}$$

When the acceptors exist in the system, eq 3 changes as follows.

$$D(t) = D(0)\exp\left[\frac{-(c_E + c_a)Bt^\alpha}{\alpha} - \frac{t}{\tau_d}\right] \tag{7}$$

where c_a is the acceptor concentration. Similarly, the number of excited acceptors, $A(t)$, is written as follows:

$$dA(t)/dt = c_a\nu(t)D(t) - A(t)/\tau_a \tag{8}$$

where τ_a is the lifetime of the acceptor. Then we obtained $A(t)$ as follows:

$$A(t) = D(0)c_a\exp\left(\frac{-t}{\tau_a}\right)\left[\int_0^t BT^{\alpha-1}\exp\left\{\frac{-(c_E + c_a)Bt^\alpha}{\alpha}\right\}\times \exp\left(\frac{T}{\tau_a}\right)dT\right] \tag{9}$$

When the donor phosphorescence overlaps the acceptor phosphorescence at a monitored wavelength, the decay profiles of the phosphorescence, $I_2(t)$, are given by the sum of the donor and acceptor phosphorescence.

$$I_2(t) = yD(0)c_a\exp\left(\frac{-t}{\tau_a}\right)\left[\int_0^t BT^{\alpha-1}\exp\left\{\frac{-(c_E + c_a)Bt^\alpha}{\alpha}\right\}\times \exp\left(\frac{T}{\tau_a}\right)dT\right] + (1-y)D(t) \tag{10}$$

where y is a fraction of the acceptor phosphorescence.

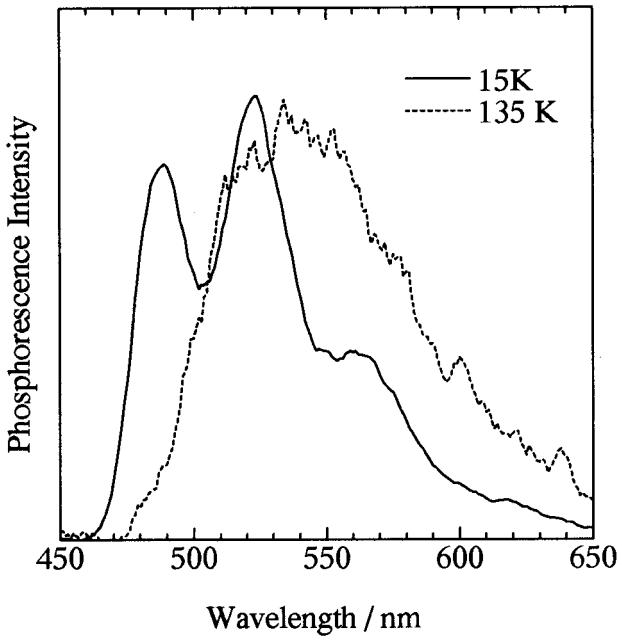

Figure 7. Time-resolved phosphorescence spectra of P(PhenMMA-*co*-MMA)H films observed in the time range 241−248 ms after excitation: at 15 K (−) and 135 K (- - -). Spectra are normalized at the maximum of each spectrum peak.

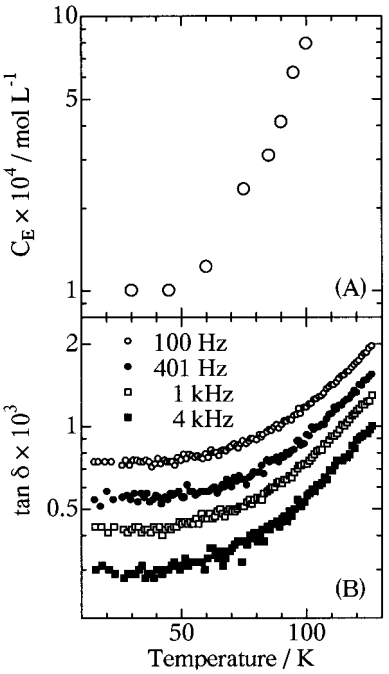

Figure 8. (A) Temperature dependence of the supertrap (excimer) concentration in P(PhenMMA-*co*-MMA)H film. (B) Dielectric loss tangent of P(PhenMMA-*co*-MMA)H at four different frequencies.

The phosphorescence decay curves of the P(PhenMMA-*co*-MMA)H films were fitted by using eq 6 with c_E, ν_0, and t_0 as the fitting parameters. We assumed that ν_0 and t_0 are independent of temperature according to Bässler's model and are fixed to 1.39×10^8 s^{-1} and 1.55×10^{-9} s, respectively. The intrinsic lifetime, τ_d, was determined by the measurement of the phosphorescence lifetime of the P(PhenMMA-*co*-MMA)L film at each temperature. The dispersion parameter, α, was calculated from the energy dispersity of the trap sites, σ, obtained previously.[39] The solid lines in Figure 3 indicate the calculated decay curves. Next, the curve fitting was performed by use of eq 10 with a fraction y for the DBN phosphorescence in P(PhenMMA-*co*-MMA)H films, where τ_a was determined by the measurement of the phosphorescence lifetime of DBN doped in PMMA films at each temperature (Table 2). Other parameters were fixed to the values that were used for the previous fitting of Phen decay curves. Figure 5 shows the results of the curve fitting as the solid lines. The calculated curves are in good agreement with the experimental ones.

What is the supertrap in the P(PhenMMA-*co*-MMA)H film? Figure 7 shows time-resolved phosphorescence spectra of the P(PhenMMA-*co*-MMA)H film at 15 and 135 K in the time range 241−248 ms after excitation. In this time range, the energy of excitons is expected to have been relaxed in the most stable distribution. At 15 K, the spectrum is attributed to the ^{3}T* phosphorescence as obtained in a photostationary condition. At 135 K, in contrast, the time-resolved phosphorescence was broad and structureless and was shifted toward the low-energy side relative to that in a photostationary condition. The spectrum at 135 K resembles that of a triplet excimer of phenanthrene that was reported previously.[40] Therefore, we assumed that the deeper trap sites, e.g., triplet excimer-forming site, act as the supertrap in the P(PhenMMA-*co*-MMA)H film.

The obtained concentration of the supertrap is shown in Figure 8A. For the poly(vinyl carbazole) film, the concentration of the excimer-forming site was estimated to be ca. 10^{-2} mol L^{-1} at 77 K,[12,41,42] which is about 2 orders of magnitude higher than the present values in the P(PhenMMA-*co*-MMA)H film.

Dielectric Relaxation. Dielectric loss tangents (tan δ) of P(PhenMMA-*co*-MMA)H film are shown in Figure 8B. Similar to the temperature dependence of c_E, tan δ increased above 50 K. The α-methyl groups in poly(alkyl methacrylate) begin to relax around this temperature.[43−45] The motion of the α-methyl groups enables the Phen chromophores to take excimer-like conformations. At a frequency higher than 4 kHz, tan δ began to increase at higher temperatures. This result indicates that the formation of a supertrap is induced by the motion of the frequency less than a few kHz.

Conclusion

Phosphorescence spectra and phosphorescence decay profiles of P(PhenMMA-*co*-MMA) films were obtained at low temperatures. Phosphorescence decay profiles of the P(PhenMMA-*co*-MMA) film with and without a triplet energy acceptor were fitted using a model in which the exciton hops among the sites having a Gaussian energy distribution. At the same temperature, both decay profiles were simulated by using the same parameters: α, ν_0, t_0, and c_E. From the simulation, the concentrations of the supertrap in P(PhenMMA-*co*-MMA)H film could be evaluated in the temperature range 30−100 K. The concentration of the supertrap showed a steep rise at around 50 K, which corresponds well to the enhancement of the matrix polymer motion observed in the dielectric measurement at a frequency of 0.1−4 kHz.

Acknowledgment. This work was supported by a Grant-in-Aid for Scientific Research on Priority Areas, Photochemical Reactions (No. 06239107) from the Ministry of Education, Science, Sports and Culture of Japan. Computation time was provided by the Supercomputer Laboratory, Institute for Chemical Research, Kyoto University. The authors are indebted to Professor Okimichi Yano, Polymer Science and Engineering, Kyoto Institute of Technology, for obtaining dielectric constants and loss factors of polymers.

References and Notes

(1) (a) Turro, N. J. *Modern Molecular Photochemistry*; Benjamin: Menlo Park, CA, 1978; p 296. (b) Birks, J. B. *Photophysics of Aromatic Molecules*; Wiley: New York, 1970; p 518. (c) Wilkinson, F. *Q. Rev.* **1966**, *20*, 403.

(2) (a) Guillet, J. E. *Polymer Photophysics and Photochemistry*; Cambridge University Press: Cambridge, U.K., 1985. (b) Soutar, I.; Phillips, D. *Photophysical and Photochemical Tools in Polymer Science*; Winnik, M. A., Ed.; Reidel: Dordrecht, The Netherlands, 1986. (c) Webber, S. C. *Polymer Photophysics*; Phillips, D., Ed.; Chapman and Hall: New York, 1985.

(3) Mort, J., Pfister, G., Eds. *Electronic Properties of Polymers*; John Wiley & Sons: New York, 1982.

(4) Webber, S. E. *Chem. Rev.* **1990**, *90*, 1469.

(5) Hoyle, C. E., Torkelson, J. M., Eds. *Photophysics of Polymers*; ACS Symposium Series 358; American Chemical Society: Washington, DC, 1987.

(6) Rabek, J. F. *Mechanisms of Photophysical Processes and Photochemical Reactions in Polymers*; John Wiley & Sons: New York, 1991.

(7) (a) Förster, Th. *Ann. Phys.* **1948**, *2*, 55. (b) Förster, Th.; Kasper, K. *Z. Elektrochem.* **1955**, *59*, 976. (c) Förster, Th. *Discuss. Faraday Soc.* **1959**, *27*, 7.

(8) Dexter, D. L. *J. Chem. Phys.* **1953**, *21*, 836.

(9) (a) Hirayama, F. *J. Chem. Phys.* **1965**, *42*, 3163. (b) Zachariasse, K.; Kühnle, W. *Z. Phys. Chem. (Munich)* **1976**, *101*, 267.

(10) Nishijima, Y. *J. Polym. Sci. C* **1970**, *31*, 353.

(11) Ito, S.; Yamamoto, M.; Nishijima, Y. *Bull. Chem. Soc. Jpn.* **1981**, *54*, 35.

(12) Klöpffer, W.; Fischer, D. *J. Polym. Sci. C* **1973**, *40*, 43.

(13) Gijzeman, O. L. J.; Langelaar, J.; Van Voorst, J. D. W. *Chem. Phys. Lett.* **1970**, *5*, 269.

(14) Itoh, Y.; Webber, S. E. *Macromolecules* **1990**, *23*, 5065.

(15) Ito, S.; Numata, N.; Katayama, H.; Yamamoto, M. *Macromolecules* **1989**, *22*, 2207.

(16) Ito, S.; Katayama, H.; Yamamoto, M. *Macromolecules* **1988**, *21*, 2456.

(17) Katayama, H.; Tawa, T.; Ito, S.; Yamamoto, M. *J. Chem. Soc., Faraday Trans. 2* **1992**, *88*, 2743.

(18) Katayama, H.; Ito, S.; Yamamoto, M. *J. Photopolym. Sci. Technol.* **1991**, *4*, 217.

(19) Vala, M. T.; Haebig, J.; Rice, S. A. *J. Chem. Phys.* **1965**, *43*, 886.

(20) (a) Yamazaki, I.; Tamai, N.; Yamazaki, T. *J. Phys. Chem.* **1990**, *94*, 516. (b) Tamai, N.; Yamazaki, T.; Yamazaki, I. *Can. J. Phys.* **1990**, *68*, 1013.

(21) Katayama, H.; Tawa, T.; Haggquist, G. W.; Ito, S.; Yamamoto, M. *Macromolecules* **1993**, *26*, 1265.

(22) El-Sayed, F. E.; MacCallum, J. R.; Pomery, P. J.; Shepherd, T. M. *J. Chem. Soc., Faraday Trans. 2* **1979**, *75*, 79.

(23) (a) Zumofen, G.; Blumen, A.; Klafter, J. *J. Chem. Phys.* **1985**, *82*, 3198. (b) Zumofen, G.; Blumen, A.; Klafter, J. *J. Chem. Phys.* **1986**, *84*, 6679.

(24) (a) Lin, Y.; Nelson, M. C.; Hanson, D. M. *J. Chem. Phys.* **1987**, *86*, 1586. (b) Lin, Y.; Dorfman, R. C.; Fayer, M. D. *J. Chem. Phys.* **1989**, *90*, 159.

(25) (a) Byers, J. D.; Friedrichs, M. S.; Friesner, R. A.; Webber, S. E. *Macromolecules* **1988**, *21*, 3402. (b) Byers, J. D.; Parsons, W. S.; Friesner, R. A.; Webber, S. E. *Macromolecules* **1988**, *21*, 3402.

(26) (a) Harmon, L. A.; Kopelman, R. *J. Phys. Chem.* **1990**, *94*, 3454. (b) Li, C. S.; Kopelman, R. *Macromolecules* **1990**, *23*, 2223.

(27) Janse van Rensburg, E. J.; Guillet, J. E.; Whittington, S. G. *Macromolecules* **1989**, *22*, 4212.

(28) Sienicki, K.; Durocher, G. *Macromolecules* **1991**, *24*, 1102.

(29) Kost, S. H.; Breuer, H. D. *Ber. Bunsen-Ges. Phys. Chem.* **1991**, *95*, 480.

(30) Mondelbrot, B. B. *The Fractal Geometry of Nature*; Freeman: San Francisco, 1982.

(31) (a) Blumen, A.; Klafter, J.; Zumofen, G. *Phys. Rev. B* **1983**, *27*, 6112. (b) Klafter, J.; Blumen, A.; Zumofen, G. *J. Stat. Phys.* **1984**, *36*, 561.

(32) Scher, H.; Lax, M. *Phys. Rev. B* **1973**, *7*, 4491. Scher, H.; Lax, M. *Phys. Rev. B* **1973**, *7*, 4502.

(33) Montroll, E. W.; Shlesinger, M. F. In *Non-Equilibrium Phenomena. II. From Stochastics to Hydrodynamics*; Lebowitz, J. L., Montroll, E. W., Eds.; North-Holland: Amsterdam, 1984; p 1.

(34) Shlesinger, M. F.; Montroll, E. W. *Proc. Natl. Acad. Sci. U.S.A.* **1984**, *81*, 1280.

(35) (a) Richert, R.; Ries, B.; Bässler, H. *Philos. Mag. B* **1984**, *49*, L25. (b) Richert, R.; Bässler, H. *J. Chem. Phys.* **1986**, *84*, 3567.

(36) Bässler, H. *Phys. Status Solidi B* **1981**, *107*, 9.

(37) (a) Schönherr, G.; Bässler, H.; Silver, M. *Philos. Mag. B* **1981**, *44*, 47. (b) Richert, R.; Elshner, A.; Bässler, H. *Z. Phys. Chem.* **1986**, *149*, 63.

(38) Katayama, H.; Tawa, T.; Haggquist, G. W.; Ito, S.; Yamamoto, M. *Macromolecules* **1993**, *26*, 1265.

(39) Hisada, K.; Ito, S.; Yamamoto, M. *J. Phys. Chem. B* **1997**, *101*, 6827.

(40) Richert, R.; Bässler, H. *Chem. Phys. Lett.* **1983**, *95*, 13.

(41) Klöpffer, W. *J. Chem. Phys.* **1969**, *50*, 2337.

(42) Klöpffer, W. *Chem. Phys.* **1981**, *57*, 75.

(43) Odajima, A.; Woodward, A. E.; Sauer, J. A. *J. Polym. Sci.* **1961**, *55*, 181.

(44) Woodward, A. E. *J. Polym. Sci. C* **1966**, *14*, 89.

(45) Shimizu, K.; Yano, O.; Wada, Y. *J. Polym. Sci., Polym. Phys. Ed.* **1975**, *13*, 1959.